Cyanidioschyzon merolae Genome. A Tool for Facilitating Comparable Studies on Organelle Biogenesis in Photosynthetic Eukaryotes[1][w]

Osami Misumi, Motomichi Matsuzaki, Hisayoshi Nozaki, Shin-ya Miyagishima[2], Toshiyuki Mori, Keiji Nishida, Fumi Yagisawa, Yamato Yoshida, Haruko Kuroiwa, and Tsuneyoshi Kuroiwa*

Laboratory of Cell Biology and Frontier Project Life's Adaptation Strategies of Environmental Changes, Department of Life Science, College of Science, Rikkyo (St. Paul's) University, Toshima, Tokyo 171–8501, Japan (O.M., S.M., T.M., Y.Y., H.K., T.K.); and Department of Biomedical Chemistry, Graduate School of Medicine (M.M.), and Department of Biological Sciences, Graduate School of Science (H.N., K.N., F.Y.), University of Tokyo, Bunkyo, Tokyo 113–0033, Japan (M.M.)

The ultrasmall unicellular red alga *Cyanidioschyzon merolae* lives in the extreme environment of acidic hot springs and is thought to retain primitive features of cellular and genome organization. We determined the 16.5-Mb nuclear genome sequence of *C. merolae* 10D as the first complete algal genome. BLASTs and annotation results showed that *C. merolae* has a mixed gene repertoire of plants and animals, also implying a relationship with prokaryotes, although its photosynthetic components were comparable to other phototrophs. The unicellular green alga *Chlamydomonas reinhardtii* has been used as a model system for molecular biology research on, for example, photosynthesis, motility, and sexual reproduction. Though both algae are unicellular, the genome size, number of organelles, and surface structures are remarkably different. Here, we report the characteristics of double membrane- and single membrane-bound organelles and their related genes in *C. merolae* and conduct comparative analyses of predicted protein sequences encoded by the genomes of *C. merolae* and *C. reinhardtii*. We examine the predicted proteins of both algae by reciprocal BLASTP analysis, KOG assignment, and gene annotation. The results suggest that most core biological functions are carried out by orthologous proteins that occur in comparable numbers. Although the fundamental gene organizations resembled each other, the genes for organization of chromatin, cytoskeletal components, and flagellar movement remarkably increased in *C. reinhardtii*. Molecular phylogenetic analyses suggested that the tubulin is close to plant tubulin rather than that of animals and fungi. These results reflect the increase in genome size, the acquisition of complicated cellular structures, and kinematic devices in *C. reinhardtii*.

To date, the genomes of more than 200 prokaryotes and several eukaryotes, including an alga, fungi, plants, animals, and their parasites, are known. However, we have little insight into the genomes of photosynthetic eukaryotes, such as *Chlamydomonas reinhardtii*, which are evolutionary intermediate organisms between primitive alga (*Cyanidioschyzon merolae*) and higher plants (Arabidopsis [*Arabidopsis thaliana*] and *Oryza sativa*), although such information would prove invaluable for investigations of the fundamental traits, origin, and evolution of eukaryotic and plant cells.

The primitive red alga *C. merolae* is a small (1.5 μm in diameter) organism that lives in sulfate-rich hot springs (pH 1.5, 45°C; De Luca et al., 1978). It has many characteristics that make it an ideal organism for elucidating the function, biosynthesis, and multiplication of organelles in eukaryotic cells. Figure 1 summarizes the dynamic changes in fine structures during mitosis in *C. merolae* compared with typical eukaryotic cells. A detailed description of the behavior and genes of each organelle will be shown in "Results and Discussion." Although a typical eukaryotic cell contains one nucleus, it has many double membrane-bound (nucleus, mitochondria, and plastids) and single membrane-bound organelles (endoplasmic reticulum [ER], Golgi apparatus, microbodies, and lysosomes), division of which occurs at random and cannot be synchronized. In addition, the shape of organelles is very diverse and complicated (Kuroiwa, 1998; Kuroiwa et al., 1998a). On the other hand, the *C. merolae* cell does not have a cell wall and contains only one nucleus, one mitochondrion, and one plastid, which are simply spherical or disc-like in shape, division of which can be completely synchronized by light treatment (Terui et al., 1995). It is also a eukaryote with one of the smallest genomes, containing minimal ultrastructural constituents of eukaryotic cells: one microbody

[1] This work was supported by grants-in-aid for Scientific Research on Priority Areas (C) Genome Biology from the Ministry of Education, Culture, Sports, Science, and Technology of Japan (nos. 1320611 and 14204078 to T.K.), and grants-in-aid from the Promotion of Basic Research Activities for Innovative Biosciences (ProBRAIN to T.K.).

[2] Present address: Department of Plant Biology, Michigan State University, East Lansing, MI 48823.

* Corresponding author; e-mail tsune@rikkyo.ne.jp; fax 81–3–3985–4592.

[w] The online version of this article contains Web-only data.

Article, publication date, and citation information can be found at www.plantphysiol.org/cgi/doi/10.1104/pp.104.053991.

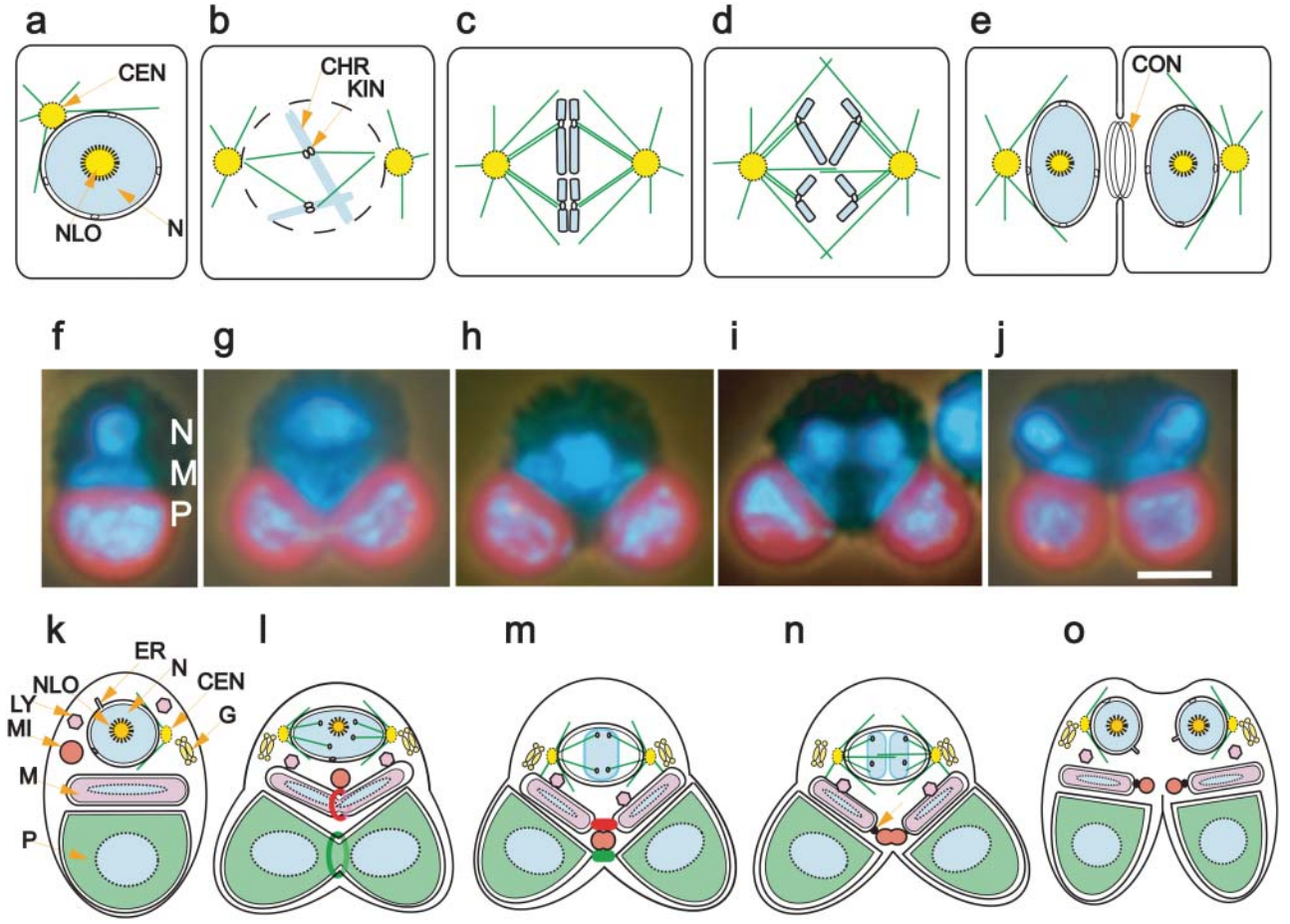

Figure 1. The basic courses of mitosis in a typical eukaryotic cell and unicellular red alga (*C. merolae*) cell. As typical cells contain many double membrane- and single membrane-bound organelles, they are not illustrated. During interphase, the centrosome (CEN) forms outside the nucleus (N), including the nucleolus (NLO; a). At prophase, the centrosome divides, and the resulting two asters can be seen to have moved apart. The chromosomes then condense; each chromosome consists of paired chromatids (CHR) attached by their kinetochores (KIN), the nuclear envelope breaks down, and the nucleolus dissolves (b). At metaphase, all the chromosomes align at the equator of the spindle (c). At anaphase, sister chromatids all separate synchronously and under the influence of microtubules, and the daughter chromosomes begin to move toward the poles (d). At telophase, the daughter nuclei and nucleolei reform using the contractile ring (CON); cytokinesis is almost complete (e). Phase contrast-fluorescent images of *C. merolae* interphase (f) and dividing cells (g–j) showing localization of nuclear (N), mitochondrial (M), and plastid DNA (P in blue/white) after 4′,6-diamidino-2-phenylindole staining are shown. The plastids emit red autofluorescence. Division of the plastid, mitochondrion, and nucleus occur in this order (f–j). During late G_2 (f) and prophase (g), the plastid and mitochondrial divisions advance and finish by the metaphase (h). At anaphase, the chromatids begin to move toward the poles, but each chromatid cannot be identified (i). Chromosomes do not condense during mitosis. Cytokinesis starts from the plastid side and closes between daughter nuclei (j). Scale bar in j = 1 μm. Schematic representation of *C. merolae* interphase (k) and dividing cells (l–o) containing single membrane-bound organelles (ER, a Golgi apparatus [G], lysosomes [LY], and a microbody [MI]) and double membrane-bound organelles (a nucleus [N], a mitochondrion [M], and a plastid [P]). The nucleus has a nucleolus (NLO), while the mitochondrion and plastids contain mitochondrial and plastid nuclei (nucleoids) in the center (blue), respectively. During interphase, the centrosome forms the focus for the interphase microtubule array outside the nucleus (k). By early prophase, the centrosome and Golgi apparatus divide, and the resulting two asters and Golgi apparatus can be seen to have moved apart (l). Chromosomal condensation does not occur during prophase. At prometaphase, the nuclear envelope does not break down. Plastid and mitochondrial divisions start in this order in late G_2 and end by metaphase. The dynamic trio (FtsZ ring, MD/PD rings, and dynamin ring) controls mitochondrial and plastid divisions. The outer MD ring (red ring in l) and outer PD ring (green in l) are illustrated at the equator of a dividing V-shaped mitochondrion and dumbbell-shaped plastids, respectively (l). Microbody and lysosomes associate with the dividing V-shaped mitochondrion (l). At metaphase and early anaphase, the bipolar structure of the spindle is clear, and all chromosomes appear to be aligned at the equator of the spindle (l). But each chromosome cannot be identified (l). Plastid and mitochondrial divisions finish by metaphase, at which time division of the microbody starts (l). The connecting bridge (arrow in n) between daughter mitochondrion and a microbody appears to play an important role in microbody division. At anaphase, sister chromatids separate synchronously, and daughter chromosomes begin to move toward the poles. Chromosomal condensation never occurs during mitosis in *C. merolae.* At telophase, the daughter nuclei and nucleoli reform, and division of the microbody might occur through the connecting bridge. By late telophase, cytokinesis is almost complete (o). The mitochondrion, lysosome, and microbody behave as if they are linked. At the final stage of cell division, a tiny contractile-like ring appears at the equator of the cell.

(peroxisome), one Golgi apparatus with two cisternae and coated vesicles, one ER, a few lysosome-like structures, and a small volume of cytosol (Kuroiwa et al., 1994). Therefore, it is very easy to determine the behavior of organelles during the cell cycle. As for the cellular mechanisms studied using *C. merolae*, for example, the role of ftsZ or dynamin in organelle division, they are common to both higher animals and plants. The simple characteristics of this alga are sure to provide an understanding of the basic mechanisms of other organelle division. This cell therefore offers unique advantages as a model organism for studies on mitochondrial and plastid divisions (Kuroiwa, 1998; Kuroiwa et al., 1998a; Miyagishima et al., 2003; Nishida et al., 2003).

The Cyanidioschyzon Genome Project was launched in 2001 with rough karyotyping (14–17 chromosomes) based on pulsed-field gel electrophoresis (Takahashi et al., 1995), using the 9 nuclear-coded genes known then. Whole-genome shotgun analyses showed the 16,520,305-bp sequence of the 20 chromosomes of *C. merolae* and allowed identification of the 5,331 genes on them. Now we have complete (100%) sequences of the *C. merolae* nuclear genome without gaps (H. Nozaki, O. Misumi, M. Matsuzaki, H. Takano, S. Maruyama, K. Tanaka, K. Terasawa, N. Sato, T. Mori, K. Nishida, F. Yagisawa, Y. Yoshida, H. Kuroiwa, and T. Kuroiwa, unpublished data). We performed annotation of the predicted genes and a genome-based evaluation of the relationship between *C. merolae* and other organisms. Consequently, we obtained complete information on all three genome compartments, nuclear (Matsuzaki et al., 2004), mitochondrial (Ohta et al., 1998), and plastid (Ohta et al., 2003), of this simple photosynthetic eukaryote.

Genome-wide analyses of this alga have provided an understanding of genes related to organelle biogenesis, multiplication, maintenance, and the ways in which progress is modulated as light conditions change. Therefore, *C. merolae* genome information will allow us to elucidate basic cellular properties common to all eukaryotes. On the other hand, genome information including approximately 25,500 genes in the approximately 115-Mb nuclear genome of the higher plant Arabidopsis is already available for many plant fields. However, *C. merolae* is markedly different from Arabidopsis taxonomically and with regards to genome size. To understand the fundamental aspects of photosynthetic organisms, before undertaking comparative genome analyses of both organisms, we need comparable genome information of intermediate organisms between *C. merolae* and Arabidopsis. The unicellular green alga *C. reinhardtii* contains an approximately 100-Mb nuclear genome, plastid genome, and mitochondria genome (Table I), and has been widely used as a model system for studying the molecular and genetic mechanisms of a number of cellular processes, such as photosynthesis, motility, and sexual reproduction (Harris, 1989).

Since *C. reinhardtii* is equipped with characteristics of cells, such as flagellar movement, and since it is capable of mating, both of which are not seen in *C. merolae*, it is very interesting to compare the genomes of both species. Genome information will provide unprecedented opportunities for plant improvements by establishing the detailed structures of and relationships between the genomes of *C. merolae* and *C. reinhardtii*. In this report, *C. merolae* is handled as a model organism of organelle research, and its intracellular structure is classified as follows: double membrane-bound organelles, single membrane-bound organelles, and cytosolic components; they are explained in terms of organelle maintenance.

RESULTS AND DISCUSSION

C. merolae was compared with typical eukaryotes, including *C. reinhardtii* and Arabidopsis, with regards to behavior of organelles during mitosis in maintaining double membrane-bound organelles, single membrane-bound organelles, and cytosolic components, which are essential for eukaryotic cells (Fig. 1). As the typical eukaryotic cell contains too many cytoplasmic double membrane- and single membrane-bound organelles, it is difficult to illustrate their behavior. By contrast, as the cell nucleus contains a large amount of DNA, the behavior of the chromosomes is well known in mitosis (Fig.1, a–e). During interphase, the centrosome forms outside the nucleus. At prophase, the centrosome divides, and the resulting two asters can be seen to have moved apart. Chromosomes then condense (each chromosome consists of paired chromatids attached by kinetochores), the nuclear envelope breaks down, and the nucleolus dissolves. At metaphase, the bipolar structure of the spindle is clear, and all chromosomes are aligned at the equator of the spindle. At anaphase, sister chromatids separate synchronously, and through microtubules, daughter chromosomes begin to move toward the poles. At telophase, the daughter nuclei and their nucleolei reform using the actin contractile ring; cytokinesis is almost complete.

Figure 1, f to j, shows phase contrast-fluorescent images of the *C. merolae* interphase and dividing cells exhibiting localization of the cell nucleus, and mitochondrial and plastid nuclei (nucleoids) after 4′,6-diamidino-2-phenylindole staining. Divisions of the plastid, mitochondrion, and nucleus occur in this order and can be highly synchronized by light/dark cycles. During late G_2, plastid and mitochondrial divisions start and finish by metaphase. At prophase, condensation of the 20 chromosomes does not occur, thus each chromosome cannot be identified during the metaphase and anaphase. Cytokinesis starts from the plastid side and closes between daughter nuclei.

As the *C. merolae* cell contains a minimal set of small membrane-bound organelles, it is easy to determine the behavior of organelles during the cell cycle. Figure 1, k to o, shows the behavior of organelles during

Table I. *Comparison of cellular components of C. merolae and C. reinhardtii*

	C. merolae	*C. reinhardtii*
Cell diameter	1–2 μm	5–10 μm
Cell division	Binary fission	Endospore division
Double membrane bounded		
Nucleus		
Chromosome number	20	19 (linkage groups)
Ploidy	Haploid	Haploid, diploid
Genome size	16.5 Mb	100 Mb
Telomeric repeat	AATGGGGGG	TTTTAGGG
Nucleolus	+	+
Chromatin, dispersed	+	+
Chromatin, condensed	+	+
Nuclear envelope	+	+
Nuclear pore	+	+
Metaphase chromosomes	Dispersed	Condensed
Mitotic spindle with microtubule	Internuclear	Internuclear
Meiosis	Unclear	+
Mitochondria		
Number per cell	1	1∼
Nucleoids	Centrally located	Centrally located
Genome	Circular	Linear
Genome size	32,221 bp[a]	15,758 bp[b]
Shape	Erythrocyte shaped	Oval, elongated, branching
Dynamics	Binary division	Division, fusion
Plastid		
Number per cell	1	1
Nucleoids	Centrally located	Dispersed
Genome	Circular	Circular
Genome size	149,987 bp[c]	203,828 bp[d]
Shape	Spherical	Cup shaped
Thylakoid	Single layer	Double layer with glana
Pyrenoid	No	1
Eyespot	No	2–4 layers
Dynamics	Binary division	Binary division
Starch granules	Cytoplasm	Stroma
Single membrane bounded		
ER	+	+
Golgi apparatus	1	10∼
Microbody	1	A few
Lysosome	2	Several
Contractile vacuole	No	2
Cell motility	Unclear	Two flagella
Cell wall	No typical wall	Cellulosic wall
Sexual reproduction	Unclear	Mating type +, −
Mating structure	No	+

[a]Ohta et al. (1998). [b]Vahrenholz et al. (1993). [c]Ohta et al. (2003). [d]Maul et al. (2002).

mitosis, obtained using data from this and previous experiments. The interphase and dividing cells contain single membrane-bound organelles (ER, one Golgi apparatus, lysosomes, and one microbody) and double membrane-bound organelles (one cell nucleus, one mitochondrion, and one plastid). The cell nucleus has a nucleolus, whereas the mitochondrion and plastids contain mitochondrial and plastid nuclei, respectively. During interphase, the centrosome forms the focus for the interphase microtubule array outside the cell nucleus. By early prophase, the centrosome and Golgi apparatus divide, and the resulting two asters and Golgi apparatus can be seen to have moved apart. Chromosomal condensation does not occur during prophase. At prometaphase, the nucleolus is dissolved but the nuclear envelope does not break down. Cell nuclei, centrosomes, ER, and Golgi apparatus behave as if they are linked. Plastid and mitochondrial divisions start in this order in G_2 and finish by metaphase. During mitochondrial and plastid divisions, a mitochondrial-dividing ring (MD ring) and plastid-dividing ring (PD ring) appear at the equator of dividing V-shaped mitochondrion and dumbbell-shaped plastids, respectively. The microbody and lysosomes associate with the dividing V-shaped mitochondrion and separate into daughter cells. At metaphase and

early anaphase, the bipolar structure of the spindle is clear, and all chromosomes appear to be aligned at the equator of the spindle, but each chromosome cannot be identified. Plastid and mitochondrial divisions finish by metaphase, at which point separation of the microbody starts. The batch-like connection between daughter mitochondrion and the microbody appears to play an important role in microbody division. At anaphase, sister chromatids begin to move toward the poles, but chromosomal condensation doesn't occur during mitosis. At telophase, the daughter nuclei and nucleoli reform, and division of the microbody finishes using the patch. By late telophase, cytokinesis is almost complete. The mitochondrion, lysosome, and microbody behave as if they are linked. It seems that there are connections between daughter mitochondria and the spindle, as if the nuclear family has a relationship with the mitochondrial family. Cytokinesis starts from the plastid side and closes between daughter nuclei. At the final stage of cell division, a tiny contractile-like ring appears at the equator of the cell. When the *C. merolae* cell was compared with typical eukaryotic cells, there were remarkable differences in condensation of chromosomes and the contractile ring for cytokinesis. Thus, detailed comparison of the structural basis between *C. merolae* and a typical photosynthetic unicellular microorganism is essential.

Table I summarizes the detailed comparison of the *C. merolae* and *C. reinhardtii* cells with regards to the fine structure and genes for maintaining double membrane-bound organelles, single membrane-bound organelles, and cytosolic components, which are essential for eukaryotic cells. There were interesting characteristics common to all as well as differences between, as shown following each organelle in the table.

Figure 2 summarizes the repertoire of *C. merolae* proteins on the basis of their assignment to eukaryotic clusters of orthologous groups (KOGs). Of the 4,771 predicted proteins, 2,536 were assigned to KOGs by emulating the National Center for Biotechnology Information (NCBI) KOGnitor service (http://www.ncbi.nlm.nih.gov/COG/new/kognitor.html). The prepublication draft sequence (*C. reinhardtii* version 2.0 gene model) and annotation data of *C. reinhardtii* used in these analyses are preliminary and might contain errors. The data of *C. reinhardtii* (gene model version 2.0) were also assigned by the same method. The distribution of the functional classification of *C. merolae* was compared with that of *C. reinhardtii* and Arabidopsis, which have similar genome size (100 Mb); in

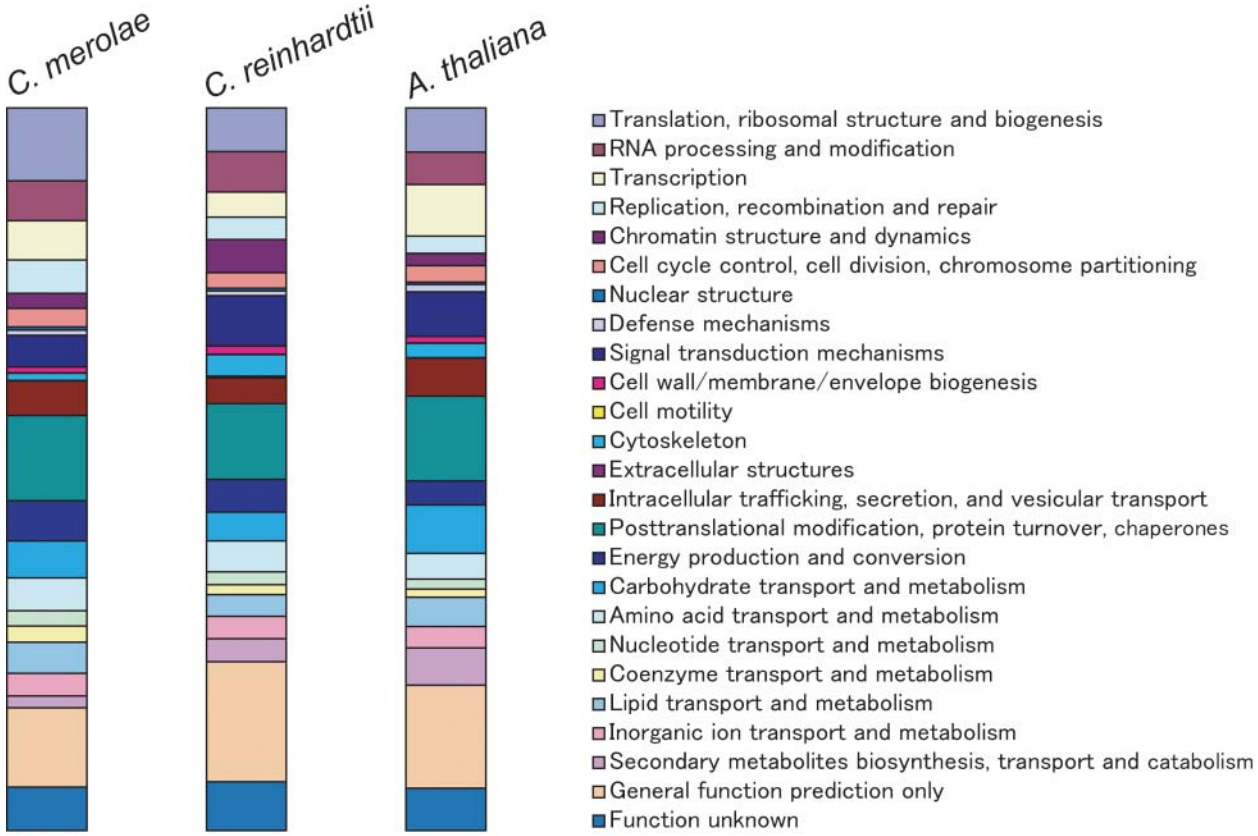

Figure 2. Comparison of the functional classification of *C. merolae* proteins with those of other organisms. Columns represent the proportion of proteins assigned to the KOG classification of each organism; *C. merolae, C. reinhardtii,* and Arabidopsis in a left-to-right fashion.

general, the distribution was similar to both species. The lowered proportion of genes for carbohydrate transport and metabolism and for secondary metabolite biosynthesis, transport, and catabolism found in the unicellular algae compared with Arabidopsis might reflect their simple cellular organization.

Compared with *C. reinhardtii* and Arabidopsis, the ratio of genes for information storage and processing is relatively large in *C. merolae* (Fig. 2). Since the entire *C. merolae* genome did not undergo gene duplication, it is thought that duplication of gene clusters, other than genes for information storage and processing, occurred in Arabidopsis. In addition, it became clear that *C. merolae* has relatively few signal transfer and cytoskeleton genes compared with *C. reinhardtii* and Arabidopsis. The gene lists and general functions of the plastids, such as respiration and photosynthesis, in *C. reinhardtii* can be found at the U.S. Department of Energy Joint Genome Institute (JGI) Web site (http://genome.jgi-psf.org/cgi-bin/metapathways?db=chlre2). In *C. merolae* and *C. reinhardtii*, the cytological features of each organelle and other components, and the related genes were compared; they are explained in the following paragraphs.

Cell Nucleus

Most eukaryotes have nucleoli that contain 100 to 1,000 tandem-repeated arrays of units encoding 18S, 5.8S, and 25S ribosomal RNA (rRNA) genes. The nucleus of *C. merolae* contains one nucleolus (Fig. 1; Kuroiwa et al., 1994) and intrinsically possesses three separate units of single ribosomal DNA (rDNA; Matsuzaki et al., 2004) distributed between different chromosomal loci (Maruyama et al., 2004). This indicates that the long tandem repeats of rDNA units, which are believed to coalesce in or around the nucleolus in most eukaryotes, are not required for nucleolar structure and innate ribosome functions in *C. merolae*. Moreover, *C. merolae* has only three copies of the 5S rRNA gene, the sequences of which are almost identical. The nucleolus structure is organized with rRNAs, small nucleolar RNAs (snoRNAs), and various associated proteins. *C. merolae* has almost 18 basic protein components, which were assigned by KOG annotation as C/D and H/ACA guide snoRNAs, respectively (Table II). These proteins are essential for growth and snoRNA accumulation in eukaryotes. Three rDNA units, a fibrillar component, and small ribonucleoproten particles colocalize and play an important role in the modification and processing of pre-rRNA. Since nucleolus-associated chromatin, as a condensed region of nucleolar DNA, is absent in *C. merolae* but develops markedly in *C. reinhardtii* compared to yeast, the *C. reinhardtii* nucleolus must have more than 150 repeats of rDNA.

The putative telomere repeats in *C. merolae* are $(AATGGGGGG)_n$, and they are found on the ends of all chromosomes; at most there are only several repeats (H. Takano, O. Misumi, S. Maruyama, M. Matsuzaki, H. Kuroiwa, and T. Kuroiwa, unpublished data). In spite of this telomere structure, the chromosomes are correctly maintained and inherited. The *C. reinhardtii* telomere repeats (Petracek et al., 1990), $(TTTTAGGG)_n$, are more A+T-rich than the *C. merolae* sequences (Table I) and are similar in sequence to higher organism such as Arabidopsis $(TTTAGGG)_n$ (Richards and Ausubel, 1998) and *Homo sapiens* $(TTAGGG)_n$ (Brown, 1989; Cross et al., 1989). In general, telomeres are separated from coding sequences by repetitive subtelomeric regions measuring several kilobases. *C. merolae* chromosomes also show multiple subtelomeric duplications; several sequence elements up to 20 kb long were duplicated at 30 of 40 putative subtelomeric regions, that is, at the terminal regions of chromosomes. In *C. reinhardtii*, the subtelomeric regions are unknown. Subtelomeric duplications have been reported in the vestigial nucleus (nucleomorph) of the cryptomonad *Guillardia theta*, which has rRNA genes and several open reading frames at both ends of all chromosomes (Douglas et al., 2001). The results support the idea that the origin of the nucleomorph might be a nucleus in a red alga.

While the centromeric region in higher eukaryotes often contains many repetitive species-specific elements and few genes, the chromosomes of *C. merolae* that were completely sequenced without gaps lack regions filled with repetitive elements (H. Nozaki, O. Misumi, M. Matsuzaki, H. Takano, S. Maruyama, K. Tanaka, K. Terasawa, N. Sato, T. Mori, K. Nishida, F. Yagisawa, Y. Yoshida, H. Kuroiwa, and T. Kuroiwa, unpublished data). Electron microscopic observations of dividing *C. merolae* cells revealed that the number of kinetochore microtubules is approximately identical to the number of chromosomes (Fig. 1; S. Maruyama, K. Nishida, and T. Kuroiwa, unpublished data). This suggests that *C. merolae* chromosomes have point or very confined centromeres, which consist of specialized nonrepetitive elements, as in *Saccharomyces cerevisiae* (Choo, 1997). We are currently in the process of determining these centromeres via immunological experiments using a centromere-specific histone H3 variant, CENP-A, which was identified in the *C. merolae* genome (S. Maruyama, H. Kuroiwa, S. Miyagishima, K. Tanaka, and T. Kuroiwa, unpublished data). Each chromosome has varying degrees of a single A+T-rich region at the midstream. Each chromosome in *C. reinhardtii* also has a point centromere (Table I; http://www.botany.duke.edu/chamy/ChlamyGen/maps.html). Since the centromeric regions are generally known to have a biased base composition, the local A+T-rich regions possibly determine the centromeres.

One of the most interesting features of *C. merolae* is each histone gene. Most eukaryotes possess multiple copies of the gene for each histone because a large amount of new histone proteins is required to make new nucleosomes in each cell cycle. *C. merolae* has one or a few genes corresponding to the histone encoded in chromosome 14 (Table II; supplemental data),

Table II. *Conserved orthologous genes of organelles in C. merolae* and *C. reinhardtii*

The reciprocal top pair of genes was shown to be orthologs as a result of BLAST analyses. When there were paralogous genes, two or more IDs are indicated in the column, and the corresponding orthologous gene is in bold. In cases of many paralogous genes (more than five), the number of genes is shown in parentheses, and the ID is indicated in supplemental data. The gene without the E-value was used to judge the relationship based on annotation.

Description	KOG No.	*C. merolae* Gene ID	*C. reinhardtii* Protein ID	E-Value
Double membrane-bound organelles				
Nucleus				
Nucleolus				
Nucleolar protein NOL1/NOP2	KOG1122	CMP349C, **CMT214C**	155441, 157957, **161814**, 163585	8.70E-33
Ribosome biogenesis protein Nop56p/Sik1p	KOG2573	CMQ185C	154535	6.00E-114
Ribosome biogenesis protein Nop58p/Nop5p	KOG2572	CMT605C	156639	1.00E-113
60S ribosomal protein 15.5 kD/SNU13, NHP2/L7A family	KOG3387	CMP335C	169550	1.40E-36
H/ACA snRNP component GAR1	KOG3262	CMI184C	154459	6.30E-18
Pseudouridine synthase	KOG2529	CMM044C	159827, **165705**, 171730	9.00E-152
Box H/ACA snoRNP component	KOG3167	CMN132C	160832, **168319**	9.00E-28
H/ACA snoRNP complex, subunit NOP10	KOG3503	CMH198C		
Nucleolar protein fibrillarin NOP77 (RRM superfamily)	KOG0127	CMR019C	162436	5.20E-28
WD40 repeat nucleolar protein Bop1, involved in ribosome biogenesis	KOG0650	CMP117C	168381, **168382**	3.60E-52
Fibrillarin and related nucleolar RNA-binding proteins	KOG1596	CMN074C	167674	1.90E-90
Nucleolar RNA-associated protein (NRAP)	KOG2054	CMT453C	152756	2.40E-11
Nucleolar protein involved in 40S ribosome biogenesis	KOG2147		159619	
Predicted nucleolar protein involved in ribosome biogenesis	KOG2154	CMP203C	153823	
Cell growth-regulating nucleolar protein	KOG2186		170784	
Proliferation-associated nucleolar protein (NOL1)	KOG2360	CMQ219C	166986	
Chromatin				
Chromatin remodeling complex WSTF-ISWI, small subunit	KOG0385	CMJ200C, **CMQ363C**	155935, **166121**, 166985, 169081	
Chromatin remodeling complex SWI/SNF	KOG0386	CMH195C, CMM316C, CMJ053C, CMS028C	155069, 158183, 165564	
Chromatin remodeling protein HARP/SMARCAL1	KOG1000	CMR070C	**154676**, 155886, 162842, 162843	7.40E-30
Chromatin assembly complex 1 subunit B/CAC2	KOG1009	CMP030C	159982	3.40E-18
Retinoblastoma pathway protein LIN-9/chromatin-associated protein Aly	KOG1019		171468	
Chromatin remodeling complex WSTF-ISWI, large subunit	KOG1245	CMJ244C		
Chromatin remodeling factor subunit and related transcription factors	KOG1279	CML061C, CMM233C		
SWI-SNF chromatin remodeling complex, Snf5 subunit	KOG1649	CMT559C		
Chromatin remodeling protein, contains PHD zinc finger	KOG1973	CMQ358C	**171356**, 160490, 154083	
Chromosome maintenance				
Structural maintenance of chromosome protein 1 (SMC1)	KOG0018	CMI192C	**169433**, 153089, 155233	1.70E-54
Structural maintenance of chromosome protein 2 (SMC2)	KOG0933	CMG189C	**164464**, 169433	3.00E-154
Structural maintenance of chromosome protein 3 (SMC3)	KOG0964	CML027C	162769, 167971	

(*Table continues on following page.*)

Table II. (*Continued from previous page.*)

Description	KOG No.	*C. merolae* Gene ID	*C. reinhardtii* Protein ID	E-Value
Structural maintenance of chromosome protein 4 (SMC4)	KOG0996	CME029C	156651, 169433	
DNA repair protein RAD18 (SMC family protein)	KOG0250	CMA066C	**154558**, 154532	8.70E-69
DNA repair protein RAD50, ABC-type ATPase/SMC superfamily	KOG0962	CMQ187C	164776	8.80E-13
Structural maintenance of chromosome protein SMC5/Spr18	KOG0979	CMH246C	156651, 156652	
Regulator of spindle pole body duplication	KOG1849	CMD159C	164991	7.60E-09
Conserved protein related to condensin complex subunit 1	KOG0413	CMQ236C		
Chromosome condensation complex condensin, subunit D2	KOG0414	CMR484C	155341	7.50E-15
Chromosome condensation complex condensin, subunit G	KOG2025	CMS422C	168195	
Chromosome condensation complex condensin, subunit H	KOG2328	CMF069C	169845	
Histone				
Histone H1	KOG4012	CMN183C	152784, 154462, 166540	
Histone H2A	KOG1756	CMN170C, **CMN174C**	**161746** + [26]	2.10E-47
Histone H2B	KOG1744	**CMN145C**, CMN173C	**153803** + [24]	1.60E-31
Histone H3	KOG1745	**CMN165C**, CMN176C, CME099C	**152775** + [35]	4.10E-52
Histone H4	KOG3467	**CMN166C**, CMN169C	**161832** + [32]	5.00E-35
CENP-A	KOG1745	CME099C		
Transport				
Karyopherin (importin) α	KOG0166	CMT096C	**154475**, 157323, 166294, 168625, 171096	2.00E-136
Karyopherin (importin) β1	KOG1241	CMO056C	161223	3.20E-82
Karyopherin (importin) β3	KOG2171	CMI255C	159427, **162988**, 165758	1.90E-15
Nuclear architecture-related protein	KOG2439	CML104C	154604, **154613**, 163470	3.70E-25
Nuclear pore complex, Nup155 component	KOG1900	CMH179C	163504	1.00E-24
Nuclear pore complex, Nup98 component	KOG0845	CMB112C	157262, 164460, 164461	
Nuclear pore complex, p54 component	KOG3091		170132	
Nuclear pore complex, rNup107 component	KOG1964	CMC129C	171545	
Nuclear porin	KOG2196		167348	
Exportin 1 (Xpo1; CRM1/MSN5)	KOG2020	CMS276C	166838	0
Nuclear transport receptor KAP120	KOG1993		164435, 167577	
Nuclear transport receptor Karyopherin-β2/Transportin	KOG2023		157342	
Nuclear transport receptor RanBP16	KOG1410		160790, 160794, 163343, 163345	
Nuclear transport receptor RANBP7/RANBP8	KOG1991		166497	
Nucleolar GTPase/ATPase p130	KOG2992		156312, 158268	
Predicted importin 9	KOG2274		154841	
Ran GTPase-activating protein	KOG1909	CMG035C	154033, 156666, **165921**, 171967	6.30E-19
Small GTP-binding protein of Ran	KOG0096	CMT257C	164622	5.60E-90
Ran-binding protein RANBP1 and related RanBD domain proteins	KOG0864		163501, 163502	

(*Table continues on following page.*)

Table II. (*Continued from previous page.*)

Description	KOG No.	*C. merolae* Gene ID	*C. reinhardtii* Protein ID	E-Value
Spliceosomes				
U1 snRNP component	KOG3168		157199, 166414	
Spliceosomal protein snRNP-U1A/U2B	KOG4206		159384, 167958	
U3 snoRNP component	KOG2781		163262	
	KOG4655		163626	
	KOG2600		171407	
U4/U6 small nuclear ribonucleoprotein Prp4	KOG0272		158503, 168282, 168801	
U5 snRNP spliceosome subunit	KOG1795		162021	
U5 snRNP-specific protein	KOG0468	CMK208C	171910	4.30E-43
U6 snRNP-associated Sm-like protein	KOG1775		166844	
Splicing factor 3b, subunit 4 (U2 snRNP)	KOG0131	CME063C	158080	
Box C/D snoRNP and U4 snRNP component Snu13p	KOG3387	CMP335C	169550	1.40E-36
Thioredoxin-like U5 snRNP component dim1	KOG3414	**CMN033**C, CMS018C	158362	4.70E-22
snRNP core Sm-like protein SmX5	KOG3448	CMB130C	**156627**, 155338	1.80E-20
Mitochondria				
Translocons				
Tom20			171301	
Tom22		CMG115C		
Tom40	KOG3296	CMF062C	161559	2.60E-41
Tom70			159288	
Tim8	KOG3489	CMI216C		
Tim9			154330	
Tim10	KOG3480	CMG033C	157296	
Tim13	KOG1733	CMB148C		
Tim17	KOG1652	CMS471C	163245, 158395	5.50E-41
Tim22	KOG3225	CMS209C	163831	6.10E-15
Tim23			156509	
Tim44	KOG2580	CMJ253C	168938	1.10E-06
Tim54	KOG2832	CMN179C	164180	9.30E-43
Division				
Dynamin-related protein			171301	
Organelle division protein FtsZ		CMG115C		
Plastid				
Translocons				
Toc34		CMP284C	153364, 156483	5.80E-14
Toc64	KOG1211		156765, 157654, 165871	
Toc75		CMJ202C	170954, 165731	
Toc159	KOG1211		153364	
Tic20			155153	
Tic22		CMC181C, CMJ105C	162599	
Tic40	KOG1308		166119, 168128	
Tic62			161722	
Tic110		CMQ342C	163303	
Division				
Dynamin-related protein		CMN262C	155446	2.00E-138
Plastid division protein FtsZ		**CMS004C**, CMO089C	152672	1.10E-89
MinE			158874	
MinD			157354	
Single membrane-bound organelles				
Endoplasmic reticulum				
ER lumen protein retaining receptor	KOG3106	CMR190C	**158379**, 166543, 172038	2.10E-57
ER-to-Golgi transport protein/RAD50-interacting protein 1	KOG2218		169153	
ER vesicle integral membrane protein	KOG2729	CME060C	161292	5.20E-14

(*Table continues on following page.*)

Table II. (*Continued from previous page.*)

Description	KOG No.	*C. merolae* Gene ID	*C. reinhardtii* Protein ID	E-Value
Membrane component of ER protein translocation complex	KOG2927		164494	
Membrane protein involved in ER to Golgi transport	KOG2887		157838, 169932	
Signal recognition particle receptor, α-subunit	KOG0781	CME016C	167087	8.60E-74
Signal recognition particle receptor, β-subunit	KOG0090	CMM147C	159090	
Signal recognition particle, subunit Srp54	KOG0780	CMC066C	157035, **165958**	1.30E-49
Signal recognition particle, subunit Srp54	KOG0780	CMO152C	171457	
Signal recognition particle, subunit Srp68	KOG2460	CML086C	161743	
Signal recognition particle, subunit Srp72	KOG2376	CMQ194C	156546	
Signal recognition particle, subunit Srp19	KOG3198	CMR091C		
Vesicle coat complex AP-1, γ-subunit	KOG1062	CMF083C	167317, 171947	
Vesicle coat complex AP-1/AP-2/AP-4, β-subunit	KOG1061	CMR021C	155972, 159826, 163531, 170720	
Vesicle coat complex AP-2, α-subunit	KOG1077		168146	
Vesicle coat complex COPI, α-subunit	KOG0292	CMD156C	157180	
Vesicle coat complex COPI, β-subunit	KOG1058	CMG048C	152346	1.00E-171
Vesicle coat complex COPI, β-subunit	KOG0276	CMT617C	168412	
Vesicle coat complex COPI, ε-subunit	KOG3081	CMD014C	155710	
Vesicle coat complex COPI, γ-subunit	KOG1078	CMP053C	172054	9.00E-172
Vesicle coat complex COPI, δ-subunit	KOG2635	CMO202C	161602	1.00E-74
Vesicle coat complex COPI, ζ-subunit	KOG3343	CMN247C	154191, **155047**	7.70E-10
Vesicle coat complex COPII, GTPase subunit SAR1	KOG0077	CMT196C	160753	
Vesicle coat complex COPII, subunit SEC13	KOG1332	CMJ112C	167415	8.80E-49
Vesicle coat complex COPII, subunit SEC23	KOG1986	CMF170C	**159292**, 167991	0
Vesicle coat complex COPII, subunit SEC24/subunit SFB2	KOG1985	CMQ471C	**168655**, 170872	6.00E-112
Vesicle coat complex COPII, subunit SFB3	KOG1984	CMQ380C	157030, 161297	
Vesicle coat complex COPII, subunit SEC31	KOG0307	CMR203C	157416	
Vesicle coat protein clathrin, heavy chain	KOG0985	CMF103C	162480	
Vesicle coat protein clathrin, light chain	KOG4031		154013	
Vesicle trafficking protein Sec1	KOG1300	CMC019C	165816, 171492	
Similar to COP-coated vesicle membrane protein p24	KOG1692	CMG098C	158201	
Golgi apparatus				
Golgi proteins involved in ER retention (RER)	KOG1688	CMI263C	171623	7.00E-42
Golgi SNAP receptor complex member	KOG3251	CMS441C	171613	1.30E-09
Golgi transport complex COD1 protein	KOG0412	CMJ219C	162230	
Golgi transport complex subunit	KOG2069	CMJ171C	156760	2.00E-11
Predicted Golgi transport complex 1 protein	KOG2211		159045	
Rab GTPase interacting factor, Golgi membrane protein	KOG3103	CMQ462C	160218	3.40E-05
Late Golgi protein sorting complex, subunit Vps53	KOG2180	CMR200C	**159541**, 161878, 162144	3.30E-13
ER-to-Golgi transport protein/RAD50-interacting protein 1	KOG2218		169153	
Microbody (peroxisome)				
Peroxin-1 (Pex1)	KOG0735	CMI027C	153527	
Pex2		CMD105C		
Pex5	KOG1125	CMK124C	160889	1.30E-27
Pex6	KOG736	CML252C		
Pex7	KOG0277		158976	
Pex10	KOG0317	CMT012C	**169232**, 169243	2.10E-08
Pex11	KOG4186		159487	
Pex12	KOG0826	CMO084C	159483	5.80E-10
Pex14	KOG2629	CMN043C	163261	
Pex19	KOG3133	CMQ019C	168404	

(*Table continues on following page.*)

Table II. (*Continued from previous page.*)

Description	KOG No.	*C. merolae* Gene ID	*C. reinhardtii* Protein ID	E-Value
Catalase	KOG0047	CMI050C	157074	1.00E-178
Lysosome				
Vacuolar H+-ATPase V0 sector, subunit a	KOG2189	CMD095C	[6]	3.00E-167
Vacuolar H+-ATPase V0 sector, subunit c″	KOG0233	CMS332C	164229	
Vacuolar H+-ATPase V0 sector, subunit d	KOG2957	CMO274C	165689	4.40E-82
Vacuolar H+-ATPase V0 sector, subunits c/c′	KOG0232	CMQ323C	159570	3.00E-40
Vacuolar H+-ATPase V1 sector, subunit A	KOG1352	CMS342C	156435	0.00E+00
Vacuolar H+-ATPase V1 sector, subunit B	KOG1351	CMP123C	167663	0
Vacuolar H+-ATPase V1 sector, subunit C	KOG2909	CMC151C	169514	2.00E-35
Vacuolar H+-ATPase V1 sector, subunit D	KOG1647	CMD007C	160328	1.90E-44
Vacuolar H+-ATPase V1 sector, subunit E	KOG1664	CMQ010C	153341	2.20E-23
Vacuolar H+-ATPase V1 sector, subunit F	KOG3432	CMQ237C	167983	8.20E-22
Vacuolar H+-ATPase V1 sector, subunit G	KOG1772	CMH200C	156178	4.60E-05
Vacuolar H+-ATPase V1 sector, subunit H	KOG2759	CMQ386C	164977	6.70E-26
Vacuolar-type H+-translocating inorganic pyrophosphatase		CMO102C	171094	8.00E-110
Lysosomal and prostatic acid phosphatases	KOG3720	CMM328C, CMT279C		
Autophagy				
Protein conjugation factor involved in autophagy	KOG3439		153015	
Ser/Thr-protein kinase involved in autophagy	KOG0595		152640, 160575, 171024	
Beclin-like protein (Apg6p)	KOG2751		163837	
Microtubule-associated anchor protein	KOG1654		168349	
Cys protease required for autophagy, Apg4p/Aut2p	KOG2674		166084	
Protein involved in autophagocytosis during starvation	KOG2981		162469	
Cytosolic components				
Actin	KOG0676	CMM237C	154863	0
Actin-related proteins	KOG0676	CMS412C, CML073C	156929, 161626, 169503, 169991	
Actin-related protein Arp4p/Act3p	KOG0679	CMR270C, CMJ223C	169502	
Actin-related protein Arp6p	KOG0680	CMS185C		
λ-Tubulin	KOG1376	CMT504C	**154911**, 164620, 165702	0
β-Tubulin	KOG1375	CMN263C	**169905**, 170055, 158210, 157194	0
γ-Tubulin	KOG1374	CMN304C	**158831**, 164724	3.00E-131
Dynein light chain type 1	KOG3430	CMT356C	**15928**, 164296, 164722	2.20E-30
Dyneins, heavy chain	KOG3595		[24]	
Kinesin (KAR3 subfamily)	KOG0239	CMR497C	152572, 154712, 166493, **168983**	6.00E-94
Kinesin (KAR3 subfamily)	KOG0239	CMT097C	168558	3.70E-87
Kinesin (SMY1 subfamily)	KOG0240		152501, 169875, 171909	
Kinesin light chain	KOG1840		[9]	
Kinesin-like protein	KOG0247		169655	
Kinesin-like protein	KOG0246		169327	
Kinesin-like protein	KOG0244		154733, 158290, 161552, 163582, 167216	
Kinesin-like protein	KOG0243		161485, 164385, 166682	
Kinesin-like protein	KOG0242	CMQ429C	[6]	
Kinesin-like protein	KOG4280	CMO070C	[13]	
Myosin class II heavy chain	KOG0161		[7]	

(*Table continues on following page.*)

Table II. (*Continued from previous page.*)

Description	KOG No.	*C. merolae* Gene ID	*C. reinhardtii* Protein ID	E-Value
Myosin class V heavy chain	KOG0160		166295, 166465, 168960, 169141	
Cell wall				
Ankyrin	KOG4177	CME092C, CMQ294C, **CMS172C**	163973 + [21]	1.30E-21
dTDP-Glc 4-6-dehydratase/UDP-GlcUA decarboxylase	KOG1429	CME136C	163641	3.00E-116
GDP-Man pyrophosphorylase	KOG1322	CMF136C	154457, 164593, 166665, 167020, 169713	
Glucosamine-6-P synthetases	KOG1268	CMK166C	158640	5.20E-80
Glucosamine-P *N*-acetyltransferase	KOG3396	**CMS020C**, CMN031C	154203	4.30E-16
Glucosidase II catalytic (alpha) subunit	KOG1066	**CMM082C**, CMM202C, CMF121C	**164756**, 164757	8.70E-59
Glycosyltransferase	KOG1387	CMI301C	153778	8.10E-16
Glycosyltransferase	KOG0853	CMT168C	156129	1.80E-28
GPI transamidase complex, GPI16/PIG-T component	KOG2407		156643	
GPI transamidase complex, GPI17/PIG-S component	KOG2459		162068	
N-Acetylglucosaminyltransferase complex, subunit PIG-A/SPT14	KOG1111	**CMR015C**, CMR346C	159722, 159723, **161264**, 168304	2.20E-77
Phospholipid scramblase	KOG0621	CMN259C	161838	2.50E-22
UDP-Glc 4-epimerase/UDP-sulfoquinovose synthase	KOG1371	CMA041C	160401	3.00E-105
UDP-Glc 4-epimerase/UDP-sulfoquinovose synthase	KOG1371	CMR012C	168872	1.20E-81
UDP-Glc 4-epimerase/UDP-sulfoquinovose synthase	KOG1371	CMR075C	152613	2.30E-80

whereas *C. reinhardtii* has many histone genes and their nuclei contain dense and dispersed chromatin (Tables I and II). The results show that the formation of chromatin does not depend on the number of histone genes. Detailed analysis of the primary structure of chromosome 14 is now under way (K. Terasawa, O. Misumi, H. Kuroiwa, T. Kuroiwa, and N. Sato, unpublished data). In *C. reinhardtii*, there are many histone genes (Table II).

C. merolae has a nuclear pore (Fig. 1), and nucleocytoplasmic transport is mainly carried out by members of the importin (karyopherin) B family and exportins. *C. merolae* also has core receptor components, importin a, b1, b3, and exportin1, their regulator of small GTP-binding protein Ran, and three nuclear pore complex components (nucleoporins); however, a few nuclear pore proteins and Ran binding-proteins do not exist. This insufficiency might be related to the simplicity of the nuclear pore structure (Table II). The lamin gene also is absent in *C. merolae* as well as *C. reinhardtii*, *S. cerevisiae*, and Arabidopsis (Table II).

Metaphase chromosomes are segregated into daughter nuclei by kinetochore microtubules in the spindle (Fig. 1). Mitotic spindles of many cells, including *C. reinhardtii*, are organized by centrosomes, which contain centrioles (basal bodies), and interactions between spindle microtubules and microtubule-based motor proteins play critical roles in spindle formation and function. In *C. reinhardtii*, the mitotic apparatus consists of many cytoskeletal proteins such as α-, β-, and γ-tubulins, bipolar kinesins, C-terminal kinesins, and so on (Table II). While there are many genes related to cytoskeletal proteins in *C. reinhardtii*, there are minimal in *C. merolae* (Table II), and little is known about the mechanism of chromosome separation by mitotic apparatus in *C. merolae.* Twelve genes encoding the structural maintenance of chromosome (SMC) family (condensin and cohesin), which is involved in metaphase chromosome formation, are included in the *C. merolae* genome (Table II). However, precise chromosome condensation has not been observed in this organism during mitosis (Fig. 1). These components of the SMC family probably act on segregation of the 20 chromosomes of *C. merolae*. The chromosome structure might have evolved considerably because metaphase cells showing 16 chromosomes are observed in *C. reinhardtii* (Loppes and Matagne, 1972).

Although transcribed RNAs are imported through nuclear pores, the genes of the *C. merolae* genome contain only 27 introns. The infrequent occurrence of introns is likely related to the lack of some known spliceosomal proteins. The splicing process of eukaryotic spliceosomal introns involves some essential small nuclear ribonucleoprotein (snRNP) complexes, the components of which are widely conserved among eukaryotes. *C. reinhardtii* also has all components of

spliceosomes (Table II). However, in the *C. merolae* genome, conserved protein subunits of U1 snRNP (A, C, and 70 kD) and U4/U6 snRNP were not detected, while those of U2 and U5 snRNP and all the common core components (Sm and Sm-like proteins) were (Table II). The RNA components of these snRNPs need to be identified experimentally because no reliable method is known for finding the genomic sequences of these RNAs. There are two possible explanations for the absence of some protein components related to splicing. First, there are unknown protein components for splicing that functionally replace U1A and other proteins. Second, splicing in *C. merolae* proceeds without those proteins known to be required in eukaryotic splicing, since the principal functions of snRNPs are generally mediated by the RNA components and support for their interaction is the main role of the protein components.

Mitochondria

Mitochondria contain mitochondrial nucleoids in which their own DNA molecules are organized by basic proteins, including a Grom (Kuroiwa et al., 1976; Kuroiwa, 1982; Sasaki et al., 2003; Sakai et al., 2004), divided by binary fission (Kuroiwa et al., 1977, 1998a), and distributed into daughter cells during each cell cycle. As the *C. merolae* cell has a single disc-shaped mitochondrion, division of which can be highly synchronized, it is easy to observe the course of mitochondrial division (Fig. 1); mitochondrial fusion does not occur. A mitochondrial dividing apparatus called a MD ring, which is larger than those of *Physarum polycephalum* (Kuroiwa, 1986), *Cyanidium caldarium* (Kuroiwa et al., 1998a), and *Nannochloropsis oculata* (Hashimoto, 2004), is observed at the equatorial region in *C. merolae* under electron microscopy (Kuroiwa et al., 1993, 1998b). The MD ring consists of double rings: an outer MD ring on the cytoplasmic side and an inner MD ring in the matrix. Previous studies have shown that *C. merolae* retains mitochondrial FtsZ (Takahara et al., 2000, 2001) and that the FtsZ forms a ring under the inner MD ring. Another primitive eukaryote alga, the chromophyte *Mallomonas splendens* (Beech et al., 2000), retains the use of FtsZ in mitochondrial division. Nishida et al. (2003) showed that *C. merolae* uses both FtsZ and dynamin in mitochondrial division. In summary, the FtsZ ring forms early at the site of future division, then the MD rings are formed, contraction of the equatorial region progresses, and, finally, the dynamin ring appears to form later and to function only in final separation, just before the FtsZ rings are dissolved (Fig. 1; Nishida et al., 2003). Therefore, a dynamic trio (FtsZ, MD, and dynamin rings) controls mitochondrial divisions.

However, in the cells of many eukaryotes, there are many mitochondria per cell, which divide at random. Even in unicellular eukaryotes such as yeasts and *C. reinhardtii*, mitochondrial shape changes dynamically from small spherical structures to a fused giant network during the cell cycle (Ehara et al., 1995). It is therefore difficult to sample a mitochondrial division event, thus *C. merolae* seems to be a model system for observing mitochondrial division. A large gene family consisting of more than 10 members encoding functionally diverse dynamin-related proteins for membrane pinching has been found in many eukaryotes (Miyagishima et al., 2003). *C. reinhardtii* also has orthologs of ftsZ and dynamin for mitochondrial division; however, their morphology continually changes with fusion and division throughout the cell cycle, and therefore detailed analyses of the dynamics have not been performed cytologically. It is predicted that *C. reinhardtii* has at least eight dynamin genes concerned with the severance of various membranes. The translocon of mitochondria is composed of several complexes. Tom40 of the general import pore; Tim23, Tim17, and Tim44 of the presequence translocase; Tim22 of the inner membrane insertion complex; and Tim9, Tim10, Tim8, and Tim13 of the intermembrane space complexes have been found in the *C. merolae* genome (Table II). But the import receptors Tom20 and Tom70, which mediate the initial step of mitochondrial import, have not been found, and a homolog of the second receptor, Tom22, had only a weak similarity. To show the presence/structure of the mitochondrial translocon in *C. reinhardtii*, more detailed genome information is required.

Plastids

Plastids contain plastid nucleoids, which show morphologic diversity such as centrally located plastid nucleoids, circular plastid nucleoids, and scattered plastid nucleoids; they are organized by basic protein (Kuroiwa et al., 1981; Sakai et al., 2004). Plastids divide by binary division or pleomorphic division (Kuroiwa et al., 2001; Momoyama et al., 2003). *C. merolae* contains one centrally located nucleoid surrounded by 5 to 10 concentric thylakoids with semicircular phycobilisomes, and the plastids are divided by binary division accompanied with plastid nucleoidal division (Fig. 1). The plastid nucleoid is organized with a bacterial histone-like protein, which is encoded in the plastid genome (Kobayashi et al., 2002). Plastid division (plastidokinesis) is associated with the formation of a so-called series of distinct PD rings (Mita and Kuroiwa, 1986) and a FtsZ ring (Miyagishima et al., 2003). Two plastid FtsZ genes (*FtsZ1-1* and *FtsZ1-2*), which are clustered into two phylogenetic groups, play a role in plastid division, and it was found that one dynamin gene (*Dnm2*) is encoded in the *C. merolae* genome (Miyagishima et al., 2003, 2004). Dynamin forms a third type of ring separated from the FtsZ and PD rings. Time-course experiments of plastid division using electron microscopy and immunofluorescence localization of FtsZ and CmDnm2 showed that the FtsZ ring forms before onset of constriction at the equator of dividing plastids and disassembles during the final stage of plastid constriction. The PD ring

forms at a somewhat later stage, at which time contraction at the equatorial region starts (Fig. 1). Dynamin (CmDnm2) begins to form a ring at the final stage of plastid division, and this ring cuts the bridge between daughter plastids formed by the PD ring. Thus, it appears that this dynamic trio of rings (FtsZ, PD, and dynamin) also functions in plastid division as with mitochondrial division.

Concerning plastid division, additional bacterial components, such as MinE and MinD, were not found in *C. merolae*. Thus, the FtsZ, PD, and dynamin rings were shown to have distinct functions in eukaryotic plastid division. PD ring genes are yet unknown, but finding them should be accelerated by the Cyanidioschyzon Genome Project. In *C. reinhardtii*, cup-shaped plastids contain their own DNAs and divide by binary divisions. The genes for plastid division, *FtsZ*, *Drp* (*Dnm*), *MinD*, and *MinE*, were retained in the nuclear genome of *C. reinhardtii* as well as in Arabidopsis (Table II).

Among the known translocon proteins in plastids, Toc34, Toc75, Tic110, Tic22, and Tic20 are encoded in the *C. merolae* genome, but other proteins such as Toc159, Tic40, and Tic55 are not found (Table II). These findings indicate that *C. merolae* has a prototypical translocon consisting of a minimal set of components, although the presence of additional rhodophyte-specific proteins cannot be excluded. McFadden and van Dooren (2004) discussed the origin and evolution of plastids using possible components of the plastid protein import apparatus based on genome information of *C. merolae* and other photosynthetic organisms. The *C. merolae* open reading frame CMM310C, with homology to Tic62 of higher plants, encodes 304 amino acid residues. CMM310C lacks the amino acid residues corresponding to the C-terminal region, which contains a repetitive module; this module interacts with a ferredoxin-NAD(P)(+) oxidoreductase in peas. Since the gene structure resembles the dehydrogenase of cyanobacteria, it is appropriate to think that the gene also functions as a dehydrogenase in *C. merolae*.

Standard components of photosynthesis genes were observed in *C. merolae*. Many of them (11 PSI genes and 17 PSII genes) are encoded in the plastid genome, while PsbO, P, U, and Z as well as a distant PsbQ homolog are encoded in the nuclear genome. Genes encoding the energy dissipation system involving the xanthophylls cycle (violaxanthin deepoxidase and zeaxanthin epoxidase) and PsbS as well as *ndh* genes, except for a gene encoding a homolog of cyanobacterial NADH dehydrogenase type II, are not present in *C. merolae*. On the other hand, the genes of xanthophylls cycle are all found, except the gene of violaxanthin deepoxidase, in *C. reinhardtii*.

Enzymes of the Calvin cycle in plants have been shown to be a mosaic of enzymes of cyanobacterial origin and enzymes originating from the eukaryotic host. Red algal Rubisco is known to be a product of horizontal gene transfer. The origin of other Calvin cycle enzymes is essentially identical in *C. merolae* and Arabidopsis (Matsuzaki et al., 2004). It is highly probable, therefore, that the complex and mosaic origin of Calvin cycle enzymes derived from common ancestors of green plants and red algae, and no essential changes occurred after the separation of the two lineages. If similar analysis is performed after complete data on Calvin cycle genes are determined for *C. reinhardtii*, this concept will be further supported.

Light signal transduction is critical for photoautotrophic organisms. Since the division of *C. merolae* cells is synchronized by light, an elaborate mechanism for light signal transduction must operate. For photoreceptors, several putative blue-light receptor (cryptochrome) genes were found in *C. merolae*, whereas no phytochrome-like genes were identified. Plant phytochromes are receptors of red and far-red light and have similarities with bacterial sensory His kinases. Since cyanobacteria also have ancestral phytochrome genes (Montgomery and Lagarias, 2002), *C. merolae* might have lost its phytochromes after its divergence from green plants. It should also be noted that the *C. merolae* nuclear genome encodes only one two-component His kinase candidate and no response regulators. In higher plants, many components of the bacterial two-component system are suggested as being involved in hormonal signaling and circadian oscillation regulation (Urao et al., 2000). Evidence for trimeric G protein and cAMP signaling is also missing; thus, these signal transduction mechanisms in *C. merolae* appear to be very simple, corroborating the result of KOG analysis. In various biological processes, the light signal is carrying out important roles in *C. reinhardtii*. Phototaxis is a typical cellular response to light signals in alga. Recently, the function of two rhodopsins, Chlamydomonas sensory rhodopsins A and B, as phototaxis receptors was demonstrated by in vivo analysis of photoreceptor electrical currents and motility responses (Sineshchekov et al., 2002). In addition, blue light controls the sexual life cycle of Chlamydomonas, which is mediated by phototropin, a UV-A/blue-light receptor that plays a prominent role in multiple photoresponses (Huang and Beck, 2003; Huang et al., 2004). It is noteworthy that the mechanism of light signal transduction and the effect on cells differ between *C. merolae* and *C. reinhardtii*, as both are photosynthetic alga.

The genome sequences of the plastid (149,987 bp) in *C. merolae* have been revealed (Ohta et al., 2003), and complete sequences from various plastids have been determined (e.g. Ohyama et al., 1986; Shinozaki et al., 1986). Phylogenetic analyses using multiple plastid genes from a wide range of eukaryotic lineages have also been carried out to resolve the robust phylogenetic relationships among plastids (e.g. Martin et al., 2002; Maul et al., 2002; Yoon et al., 2002; Ohta et al., 2003). Nozaki et al. (2003) reported plastid phylogeny and evolution based on a loss of plastid genes deduced from complete plastid genome sequences from a wide range of eukaryotic phototrophs. They represented a wide range of eukaryotic lineages (including three secondary plastid-containing groups) as two large monophy-

letic groups with high bootstrap values. Complete genome information of photosynthetic eukaryotes will allow elucidation of phylogenetic relationships according to the transfer of genes between genomes, as well as provide an understanding of the genetic regulation systems of photosynthesis in plastids.

Endoplasmic Reticulum

The cytoplasm of *C. merolae* contains small, coated vesicles and a rough-surface ER. The double-nuclear membrane is continuously covered with ER, and a Golgi body is usually situated nearby (Fig. 1). The alignment of these membrane systems in the cell of *C. reinhardtii* is similar, although *C. reinhardtii* has more single membrane-bound organelles per cell than *C. merolae*. Signal recognition particles on the ER play a critical role in protein sorting across the membrane. Among the known components of the signal recognition particles, the genes for SRP19, SRP54, SRP68, and SRP72 were found in the *C. merolae* genome, but the genes for SRP9 and SRP14, which are involved in translational arrest of ribosomes that synthesize signal-containing polypeptides conserved in many organisms, were not detected (Table II).

The *C. merolae* genome encodes limited subsets of vesicle-coating proteins. We were able to find suites of coatomers for COPI- and COPII-coated vesicles with key GTPases for their formation, namely Arf1 and Sar1p (Kirchhausen, 2000), respectively (Table II). We also found the heavy chain of clathrin but no obvious homolog for the light chain, which regulates the formation of clathrin triskelion and has more sequence diversity than the heavy chain. In yeasts, gene disruption of the light chain causes serious but not complete defects in clathrin-mediated transportation that can be partially rescued by overexpression of the heavy chain. It is therefore possible to assume that the light chain of clathrin might be altered in *C. merolae*. Furthermore, only one set of adaptor protein (AP) complexes for clathrin exists in *C. merolae*, whereas at least three of the four sets of subunits exist in all other eukaryotes for which genome information is available.

Golgi Apparatus

One Golgi apparatus was usually located near the centrosome in *C. merolae* (Fig. 1), whereas several were observed around the cell nucleus in *C. reinhardtii*. In both organisms, vesicles from the ER to the Golgi apparatus were observed by ultrastructural studies (Kuriyama et al., 1999). Several genes of the Golgi transport system have been annotated (Table II), but details of the vesicle transport system require clarification based on genome information.

Microbodies (Peroxisome)

Microbodies are recognized as electron dense bodies by electron microscopy. The behavior of the microbody was observed and formation of its three-dimensional structure was reconstructed from serial thin sections around one set of cell division cycle in *C. merolae* (Fig. 1; Miyagishima et al., 1998). The microbody changed shape intricately at the prophase during mitosis and then was divided by binary division. The electron dense patch-like connection between a daughter microbody and daughter mitochondria appeared to be available for separation of daughter microbodies (Fig. 1; Miyagishima et al., 2001). In addition, Pex11p, which is the key regulator of microbody division and proliferation, is present in *C. reinhardtii* but absent in *C. merolae* (Table II). Although there are genes coding most of the major proteins involved in protein sorting from the cytosol to organelles, some additional genes are lacking in *C. merolae*. Two kinds of signals (peroxisome targeting signals), PTS1 and PTS2, are known to be present in precursor proteins of microbodies. *C. merolae* has a final precursor protein receptor (Pex14p) and initial receptor protein (Pex5p) for PTS1, but lacks an obvious homolog of the PTS2 receptor (Pex7p; Table II). Catalase behaves as a catalyst for the conversion of hydrogen peroxide into water and oxygen in the microbody. *C. merolae* has a typical catalase gene, and its protein was detected in the microbody by immunoelectron microscopy (Miyagishima et al., 1999). Although such microbody-like structures appear in sections of Chlamydomonas cells, they have received relatively little experimental attention.

Lysosomes

C. merolae cells have a few lysosome-like structures, which contain lysosomal enzymes such as vacuolar ATPase, vacuolar pyrophosphatase, and acid phosphatase (Table II; F. Yagisawa, H. Kuroiwa, T. Nagata, and T. Kuroiwa, unpublished data). In mitosis, lysosomes in *C. merolae* seem to behave as a mitochondrial family (Fig. 1); the behavior and multiplication of lysosomes during the cell cycle will be reported in detail in the future (F. Yagisawa, unpublished data). None of the genes related to autophagy were found in the *C. merolae* genome, but several autophagy genes are retained in *C. reinhardtii* (Apg4, 6), yeast (Hamasaki et al., 2005), and mammalian genomes (Cuervo, 2004). Autophagy is a mechanism for optimizing the abundance of cellular components and for recycling biomolecular resources such as amino acids.

Cytosolic Components and Surface Structure

The tubulin family carries out most fundamental biological functions, such as cytoskeleton, flagella movement and chromosome separation in eukaryotic cells. In *C. merolae*, a simple spindle consisting of kinetochore microtubules, polar microtubules, and patch-like centrosome is found and was seen to play a role in the separation of the 20 chromosomes (Fig. 1). The formation, behavior, and function of the spindle will be published in detail in the future (K. Nishida, H. Kuroiwa, T. Nagata, and T. Kuroiwa, unpublished

data). The genome of *C. merolae* only includes three genes that code α-, β-, and γ-tubulin proteins, respectively, compared to nine in *C. reinhardtii* (Table II). In *C. merolae*, there are no basal bodies or flagella, but there are mitotic spindles. However, *C. reinhardtii* cells have basal bodies, flagella, and mitotic spindles. Paralogous genes corresponding to α-, β-, and γ-tubulin, respectively, have not been found in the nuclear genome of *C. merolae*. Comparative analysis of the existence of flagellar structures with the composition of tubulin genes, and their phylogenetic relationship, will be interesting in the future. To confirm the relationships between cytoskeletal or motility machinery in the *C. merolae* and *C. reinhardtii*, we examined the phylogeny of tubulin genes. A phylogenetic tree inferred from the amino acid sequences of α-, β-, and γ-tubulin from the KEGG database release 3.0 was constructed for *C. reinhardtii* (version 2.0 gene model) and *C. merolae* by the neighbor-joining (NJ) method (Fig. 3). Three major groups were distinguished for the α-, β-, and γ-groups. The gene of *C. merolae* was positioned basally to the lineage, including Arabidopsis and Plasmodium homologs in each of the three tubulin families, and the *C. merolae* β-tubulin gene was positioned with the *Encephalitozoon cuniculi* lineage. The α-, β-, and γ-tubulin genes of *C. reinhardtii*

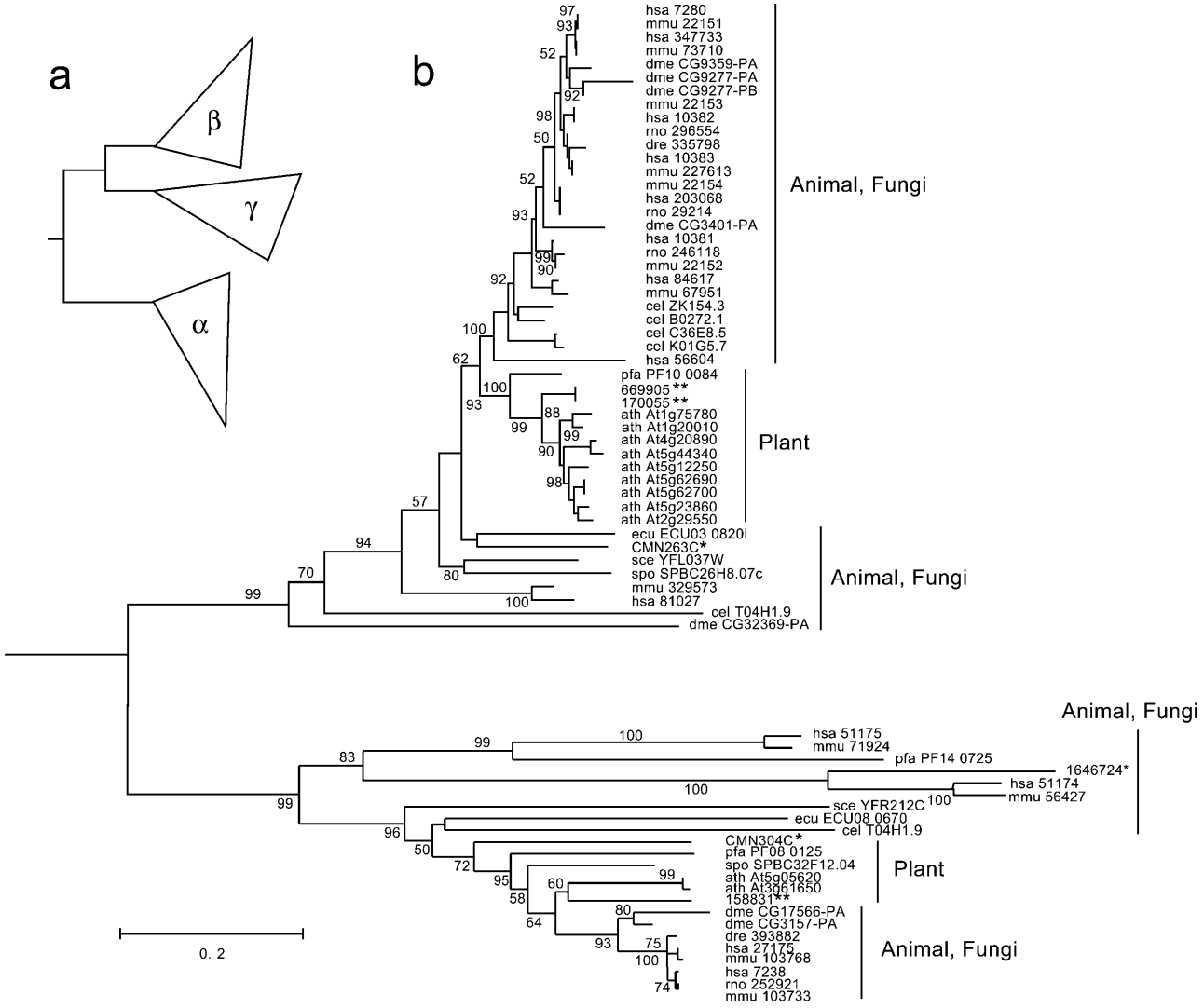

Figure 3. Schematic representation of the phylogenetic groups of tubulin (a). Phylogenetic relationships of β- and γ-tubulin genes (b) and α-tubulin genes (c). The tree was constructed by the NJ method using Kimura distances. Branch lengths are proportional to Kimura distances, which are indicated by the scale bar below the tree. Numbers at branches represent the bootstrap values (50% or more) based on 1,000 replications. The asterisk and double asterisk indicate genes from *C. merolae* gene ID and *C. reinhardtii* protein ID, respectively. The other species were shown in the abbreviations of KOG: has, *H. sapiens*; mmu, *Mus musculus*; rno, *Rattus norvegicus*; dre, *Danio rerio*; dme, *Drosophila melanogaster*; cel, *Caenorhabditis elegans*; ath, Arabidopsis; cme, *C. merolae*; cre, *C. reinhardtii*; sce, *S. cerevisiae*; spo, *Schizosaccharomyces pombe*; ecu, *E. cuniculi*; and pfa, *Plasmodium falciparum*. Each gene is described by entry number in the KEGG database according to the abbreviated species name.

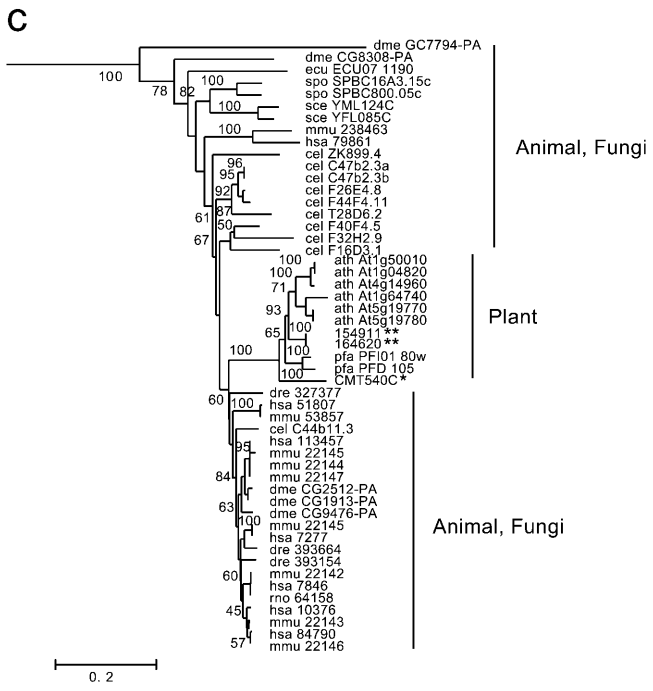

Figure 3. (*Continued.*)

were shown to be sisters of the Arabidopsis group. It is surprising that each tubulin gene of *C. reinhardtii*, which is currently widely used as a model system of flagellum equipment, showed a close relationship to a higher plant as a result of molecular phylogenetic analysis. α-, β-, and γ-tubulin genes have not been duplicated in *C. merolae* after branching with a green lineage, but α- and β-tubulin genes have been observed in *C. reinhardtii*.

In *C. merolae*, there is no particular structure outside the plasma membrane. In *C. reinhardtii*, a specialized region differentiates the narrow membrane zone overlying the plasma membrane at the cell anterior, giving rise to the fertilization tubule of the mating-type plus cells. In cross section, an electron-dense ring appears to be associated with the plasma membrane. During sexual conjugation, the fertilization tubule has been shown to contain an F-actin bundle; an actin gene defect was apparently caused by deficient growth of the fertilization tubule. One actin and several other proteins probably play a crucial role in the formation of the fertilization tubule in *C. reinhardtii* (Kato-Minoura et al., 1997). On the other hand, this structure and phenomenon were not found in *C. merolae*, which didn't express an actin gene (Takahashi et al., 1995). The absence of myosin is consistent with the fact that actin microfilaments for cytokinesis were not detected by electron microscopy or immunodetection, and that expressed sequence tag clones for the actin gene were not obtained (Matsuzaki et al., 2004). It is proposed that *C. merolae* cells do not require the actomyosin system, at least under our culture conditions; this is supported by the fact that disruption of the actomyosin system in other organisms does not necessarily cause lethality or complete cell division defectiveness. Probably, cytokinesis might be performed by a primitive contractile ring.

A typical cell wall was not observed in *C. merolae* by electron microscopy (Kuroiwa et al., 1994). The multilayered cell wall of *C. reinhardtii* consists of an insoluble Hyp-rich glycoprotein framework and several chaotrope-soluble Hyp-containing glycoproteins. Despite conservation of the genes for cell wall biosynthesis in both algae (Table II), there is no cell wall in *C. merolae*. There must therefore be a primitive, not rigid, cell surface structure in *C. merolae*. In addition to the surface structure of *C. merolae*, the existence of highly expressed transporter genes on the plasma membrane is involved in the mechanism that allows adaptation to strong acid and heavy metal ion-rich environments. The genes of cell adhesion molecules, such as integrin, cadherin, and catenin, which are conserved in animal cells, did not exist in *C. merolae*.

C. reinhardtii has two mating types that fuse to form diploid zygotes when each gamete is mixed. Uniparental inheritance of plastid DNA occurs during this sexual reproduction process (Kuroiwa et al., 1982; Nishimura et al., 2002). Although some genes involved in uniparental inheritance of *C. reinhardtii* have been reported (Ferris et al., 2002), the key gene of this phenomenon remains to be elucidated. Whole-genome information of *C. reinhardtii* will provide us with novel information about organelle inheritance and perhaps help elucidate the sex of *C. merolae*. Comparative genome analyses between *C. merolae* and *C. reinhardtii* with regards to the evolution of sexual reproduction and inheritance of organelles will be an interesting topic of study in the future.

CONCLUSION

The complete genome sequence of *C. merolae* revealed that this organism possesses unique features in its primary sequence structure and gene composition, making it useful for understanding the basic system and division of organelles and the evolution of photosynthetic eukaryotes. For understanding the maintenance of organelles, the *C. merolae* and *C. reinhardtii* genome projects provide complete or sufficient genome sequence data, which allows comparative orthologous analysis of the two algal genomes. Since it is composed of a minimum gene set, *C. merolae* genome information should accelerate studies on, for example, the establishment of cellular components, and will allow us to elucidate cellular and molecular properties common to other eukaryotes. In addition, the present genome information of *C. merolae* demonstrates the fundamental attributes of photosynthesis in eukaryotes and the unique photosynthetic features that are distinct from green phototrophs. These unique features of *C. merolae* should help provide an understanding of the origin, evolution, and fundamental structure and function of eukaryotes.

Recently, the isolation of a mutant (Yagisawa et al., 2004) and nuclear transformation by homologous recombination have been reported in *C. merolae* (Minoda et al., 2004). *C. reinhardtii* is also known to be a good model organism for studies of molecular biology with transformation techniques of plastids (Harris, 2001). There is only one report about homologous recombination of the nuclear genome, but the technique used is very complicated (Sodeinde and Kindle, 1993); the procedure is, thus, far from routine for this alga. Homologous recombination of the nuclear genome of plants has so far only been reported in the moss *Physcomitrella patens* (Schaefer, 2002). Therefore, gene-targeting technology using the unicellular *C. merolae* system will help solve many problems with regards to plant as well as basic eukaryotic biology.

Despite considerable advances in our understanding of organelle evolution and biogenesis, future proteomic and gene-targeting analyses promise to accelerate our understanding of these vital features of photosynthetic eukaryotes. Now, we have obtained complete sequences of the three genome compartments and are advancing microarray and proteome analyses as post-genome studies of *C. merolae*.

MATERIALS AND METHODS

Predicted proteins of *Cyanidioschyzon merolae* and *Chlamydomonas reinhardtii* were compared by reciprocal WU-BLASTP comparisons; that is, each predicted *C. merolae* nuclear protein was compared against all the predicted proteins of *C. reinhardtii* (JGI *C. reinhardtii* version 2.0 gene model) and vice versa. When a high-scoring pair was detected, we collected all members of the groups from both organisms. Functional classification was performed based on the NCBI eukaryotic cluster of orthologous genes by emulating the KOGnitor service (http://www.ncbi.nlm.nih.gov/COG/new/kognitor.html). Gene lists in the table were basically classified for each organelle by KOG description. The prepublication draft sequence (JGI *C. reinhardtii* version 2.0 gene model) and annotation data of *C. reinhardtii*, which were used in the analyses, are preliminary and might contain errors.

The gene lists and metabolic maps of the general functions of mitochondria and plastids, such as respiration and photosynthesis, can be found on the KEGG Web site (http://www.genome.jp/kegg/).

Phylogenetic Analyses of Tubulin Genes

The amino acid sequences of orthologous α-, β-, and γ-tubulin were extracted from the KEGG database release 3.0 and aligned using ClustalX 30 with the default option. After gaps in the alignment were excluded, the three tubulin genes of *C. merolae* were included and used for phylogenetic analysis. NJ trees based on Kimura distances were calculated using ClustalX. Bootstrap values in the NJ analysis were carried out based on 1,000 replications, also using ClustalX.

ACKNOWLEDGMENT

We thank members of *C. merolae* genome project for helpful discussion.

Received September 30, 2004; returned for revision December 16, 2004; accepted December 17, 2004.

LITERATURE CITED

Beech PL, Nheu T, Schultz T, Herbert S, Lithgow T, Gilson PR, McFadden GI (2000) Mitochondrial FtsZ in a chromophyte alga. Science **287:** 1276–1279

Brown WR (1989) Molecular cloning of human telomeres in yeast. Nature **338:** 774–776

Choo KHA (1997) The Centoromere. Oxford University Press, Oxford

Cross SH, Allshire RC, McKay SJ, McGill NI, Cooke HJ (1989) Cloning of human telomeres by complementation in yeast. Nature **338:** 771–774

Cuervo AM (2004) Autophagy: in sickness and in health. Trends Cell Biol **14:** 70–77

De Luca P, Taddei R, Varano L (1978) *Cyanidioschyzon merolae*: a new alga of thermal acidic environments. Webbia **33:** 37–44

Douglas S, Zauner S, Fraunholz M, Beaton M, Penny S, Deng LT, Wu X, Reith M, Cavalier-Smith T, Maier UG (2001) The highly reduced genome of an enslaved algal nucleus. Nature **410:** 1091–1096

Ehara T, Osafune T, Hase E (1995) Behavior of mitochondria in synchronized cells of *Chlamydomonas reinhardtii* (Chlorophyta). J Cell Sci **108:** 499–507

Ferris PJ, Armbrust EV, Goodenough UW (2002) Genetic structure of the mating-type locus of *Chlamydomonas reinhardtii*. Genetics **160:** 181–200

Hamasaki M, Noda T, Baba M, Ohsumi Y (2005) Starvation triggers the delivery of the endoplasmic reticulum to the vacuole via autophagy in yeast. Traffic **6:** 56–65

Harris EH (1989) The *Chlamydomonas* Sourcebook: A Comprehensive Guide to Biology and Laboratory Use. Academic Press, San Diego

Harris EH (2001) *Chlamydomonas* as a model organism. Annu Rev Plant Physiol Plant Mol Biol **52:** 363–406

Hashimoto H (2004) Mitochondrion-dividing ring in an alga *Nannochloropsis oculata* (Eusitigmatophyceae, Heterokonta). Cytologia (Tokyo) **69:** 323–326

Huang K, Beck CF (2003) Phototropin is the blue-light receptor that controls multiple steps in the sexual life cycle of the green alga *Chlamydomonas reinhardtii*. Proc Natl Acad Sci USA **100:** 6269–6274

Huang K, Kunkel T, Beck CF (2004) Localization of the blue-light receptor phototropin to the flagella of the green alga *Chlamydomonas reinhardtii*. Mol Biol Cell **15:** 3605–3614

Kato-Minoura T, Hirono M, Kamiya R (1997) *Chlamydomonas* inner-arm dynein mutant, ida5, has a mutation in an actin-encoding gene. J Cell Biol **137:** 649–656

Kirchhausen T (2000) Three ways to make a vesicle. Nat Rev Mol Cell Biol **1:** 187–198

Kobayashi T, Takahara M, Miyagishima S, Kuroiwa H, Sasaki N, Ohta N, Matsuzaki M, Kuroiwa T (2002) Detection and localization of a plastid-encoded HU-like protein that organizes plastid nucleoids. Plant Cell **14:** 1579–1589

Kuriyama H, Takano H, Suzuki L, Uchida H, Kawano S, Kuroiwa H, Kuroiwa T (1999) Characterization of *Chlamydomonas reinhardtii* zygote-specific cDNAs that encode novel proteins containing ankyrin repeats and WW domains. Plant Physiol **119:** 873–884

Kuroiwa H, Mori T, Takahara M, Miyagishima S, Kuroiwa T (2001) Multiple FtsZ rings in a pleomorphic chloroplast in embryonic cap cells of *Pelargonium zonale*. Cytologia (Tokyo) **66:** 227–233

Kuroiwa T (1982) Mitochondrial nuclei. Int Rev Cytol **75:** 1–59

Kuroiwa T (1986) Mitochondria multiplication with mitochondrial nucleoids division. Kagaku **56:** 339–348

Kuroiwa T (1998) The primitive red algae: *Cyanidium caldarium* and *Cyanidioschyzon merolae* as model system for investigating the dividing apparatus of mitochondria and plastids. Bioessays **20:** 344–354

Kuroiwa T, Kawano S, Hizume M (1976) A method of isolation of mitochondrial nucleoid of *Physarum polycephalum* and evidence of a basic protein. Exp Cell Res **97:** 435–445

Kuroiwa T, Kawano S, Hizume M (1977) Studies on mitochondrial structure and function in *Physarum polycephalum*. V. Behavior of mitochondrial nucleoids throughout mitochondrial division cycle. J Cell Biol **72:** 687–697

Kuroiwa T, Kawano S, Nishibayashi S, Sato C (1982) Epifluorescence microscopic evidence for maternal inheritance of chloroplast DNA. Nature **298:** 481–483

Kuroiwa T, Kawazu T, Takahashi H, Suzuki K, Ohta N, Kuroiwa H (1994) Comparison of ultrastructures between the ultra-small eukaryote *Cyanidioschyzon merolae* and *Cyanidium caldarium*. Cytologia (Tokyo) **59:** 149–158

Kuroiwa T, Kuroiwa H, Sakai A, Takahashi H, Toda K, Itoh R (1998a) The division apparatus of plastid and mitochondria. Int Rev Cytol **181:** 1–41

Kuroiwa T, Suzuki K, Kuroiwa H (1993) Mitochondrial division by an

electron-dense ring in *Cyanidioschyzon merolae.* Protoplasma **175:** 173–177

Kuroiwa T, Suzuki K, Itoh R, Toda K, Okeefe TC, Kuroiwa H (1998b) Mitochondria-dividing ring: ultrastructural basis for the mechanisms of mitochondrial division in *Cyanidioschyzon merolae.* Protoplasma **186:** 12–23

Kuroiwa T, Suzuki T, Ogewa K, Kawano S (1981) The chloroplast nucleus: distribution, number size and shape, and a model for the multiplication of the chloroplast genome during chloroplast development. Plant Cell Physiol **22:** 322–338

Loppes R, Matagne R (1972) Allelic complementation between arg-7 mutants in *Chlamydomonas reinhardtii.* Genetica **43:** 422–430

Martin W, Rujan T, Richly E, Hansen A, Cornelsen S, Lins T, Leister D, Stoebe B, Hasegawa M, Penny D (2002) Evolutionary analysis of Arabidopsis, cyanobacterial, and plastid genomes reveals plastid phylogeny and thousands of cyanobacterial genes in the nucleus. Proc Natl Acad Sci USA **99:** 12246–12251

Maruyama S, Misumi O, Ishii Y, Asakawa S, Shimizu A, Sasaki T, Matsuzaki M, Shin-i T, Nozaki H, Kohara Y, et al (2004) The minimal eukaryotic ribosomal DNA units in the primitive red alga *Cyanidioschyzon merolae.* DNA Res **11:** 83–91

Matsuzaki M, Misumi O, Shin-i T, Maruyama S, Takahara M, Miyagishima S, Mori T, Nishida K, Yagisawa F, Nishida K, et al (2004) Genome sequence of the ultrasmall unicellular red alga *Cyanidioschyzon merolae* 10D. Nature **428:** 653–657

Maul JE, Lilly JW, Cui L, dePamphilis CW, Miller W, Harris EH, Stern DB (2002) The *Chlamydomonas reinhardtii* plastid chromosome: islands of genes in a sea of repeats. Plant Cell **14:** 2659–2679

McFadden GI, van Dooren GG (2004) Evolution: Red algal genome affirms a common origin of all plastids. Curr Biol **14:** 514–516

Minoda A, Sakagami R, Yagisawa F, Kuroiwa T, Tanaka K (2004) Improvement of culture conditions and evidence for nuclear transformation by homologous recombination in a red alga, *Cyanidioschyzon merolae* 10D. Plant Cell Physiol **45:** 667–671

Mita T, Kuroiwa T (1986) Division of plastid by a plastid-dividing ring in Cyanidium cardarium. Protoplasma (Suppl) **1:** 133–152

Miyagishima S, Itoh R, Toda K, Kuroiwa H, Nishimura M, Kuroiwa T (1999) Microbody proliferation and segregation cycle in the single-microbody alga *Cyanidioschyzon merolae.* Planta **208:** 326–336

Miyagishima S, Itoh R, Toda K, Takahashi H, Kuroiwa H, Kuroiwa T (1998) Orderly formation of the double ring structures for plastid and mitochondrial division in the unicellular red alga *Cyanidioschyzon merolae.* Planta **120:** 551–560

Miyagishima S, Kuroiwa H, Kuroiwa T (2001) The timing and manner of disassembly of the apparatus for chloroplast and mitochondrial division in the red alga *Cyanidioschyzon merolae.* Planta **212:** 517–528

Miyagishima S, Nishida K, Mori T, Matsuzaki M, Higashiyama T, Kuroiwa H, Kuroiwa T (2003) A plant-specific dynamin-related protein forms a ring at the plastid division site. Plant Cell **15:** 655–665

Miyagishima S, Nozaki H, Nishida K, Nishida K, Matsuzaki M, Kuroiwa T (2004) Two types of FtsZ proteins in mitochondria and red-lineage plastids: The duplication of FtsZ is implicated in endosymbiosis. J Mol Evol **58:** 291–303

Momoyama Y, Miyazawa Y, Miyagishima S, Mori T, Misumi O, Kuroiwa H, Kuroiwa T (2003) The pleomorphic division of plastids by FtsZ in tobacco Bright Yellow-2. Eur J Cell Biol **82:** 323–332

Montgomery BL, Lagarias JC (2002) Phytochrome ancestry: sensors of bilins and light. Trends Plant Sci **7:** 357–366

Nishida K, Takahara M, Miyagishima S, Kuroiwa H, Matsuzaki M, Kuroiwa T (2003) Dynamic recruitment of dynamin for final mitochondrial severance in a red alga. Proc Natl Acad Sci USA **100:** 2146–2151

Nishimura Y, Misumi O, Kato K, Inada N, Higashiyama T, Momoyama Y, Kuroiwa T (2002) An mt^+ gamete-specific nuclease that targets mt^- chloroplasts during sexual reproduction in *C. reinhardtii.* Genes Dev **16:** 1116–1128

Nozaki H, Ohta N, Matsuzaki M, Misumi O, Kuroiwa T (2003) Phylogeny of plastids based on cladistic analysis of gene loss inferred from complete plastid genome sequences. J Mol Evol **57:** 377–382

Ohta N, Sato N, Kuroiwa T (1998) Structure and organization of the mitochondrial genome of the unicellular red alga *Cyanidioschyzon merolae* deduced from the complete nucleotide sequence. Nucleic Acids Res **26:** 5190–5198

Ohta N, Matsuzaki M, Misumi O, Miyagishima S, Nozaki H, Tanaka K, Shin-i T, Kohara Y, Kuroiwa T (2003) Complete sequence and analysis of the plastid genome of the unicellular red alga *Cyanidioschyzon merolae.* DNA Res **10:** 67–77

Ohyama K, Fukuzawa H, Kohchi T, Shirai H, Sano T, Sano S, Umesono K, Shiki Y, Takeuchi M, Chang Z, et al (1986) Plastid gene organization deduced from complete sequence of liverwort *Marchantia polymorpha* plastid DNA. Nature **322:** 572–574

Petracek ME, Lefebvre PA, Silflow CD, Berman J (1990) Chlamydomonas telomere sequences are A+T-rich but contain three consecutive G-C base pairs. Proc Natl Acad Sci USA **87:** 8222–8226

Richards EJ, Ausubel FM (1998) Isolation of a higher eukaryotic telomere from *Arabidopsis thaliana.* Cell **53:** 127–136

Sakai A, Takano H, Kuroiwa T (2004) Organelle nuclei in higher plants: structure, composition, function, and evolution. Int Rev Cytol **238:** 59–118

Sasaki N, Kuroiwa H, Nishitani C, Takano H, Higashiyama T, Kobayashi T, Sakai A, Kawano S, Murakami-Murofushi K, Kuroiwa T (2003) Glom is a novel mitochondrial DNA packaging protein in *Physarum polycephalum* and causes intense chromatin condensation without suppressing DNA function. Mol Biol Cell **14:** 4758–4769

Schaefer DG (2002) A new moss genetics: targeted mutagenesis in *Physcomitrella patens.* Annu Rev Plant Biol **53:** 477–501

Shinozaki K, Ohme M, Tanaka M, Wakasugi T, Hayashida N, Matsubayashi T, Zaita N, Chunwongse J, Obokata J, Yamaguchi-Shinozaki K, et al (1986) The complete nucleotide sequence of the tobacco plastid genome: its gene organization and expression. EMBO J **5:** 2043–2049

Sineshchekov OA, Jung KH, Spudich JL (2002) Two rhodopsins mediate phototaxis to low- and high-intensity light in *Chlamydomonas reinhardtii.* Proc Natl Acad Sci USA **99:** 8689–8694

Sodeinde OA, Kindle KL (1993) Homologous recombination in the nuclear genome of *Chlamydomonas reinhardtii.* Proc Natl Acad Sci USA **90:** 9199–9203

Takahara M, Kuroiwa H, Miyagishima S, Mori T, Kuroiwa T (2001) Localization of the mitochondrial FtsZ protein in a dividing mitochondria. Cytologia (Tokyo) **66:** 421–425

Takahara M, Takahashi H, Matsunaga S, Miyagishima S, Takano H, Sakai A, Kawano S, Kuroiwa T (2000) A putative mitochondrial ftsZ gene is present in the unicellular primitive red alga *Cyanidioschyzon merolae.* Mol Gen Genet **264:** 452–460

Takahashi H, Takano H, Yokoyama A, Hara Y, Kawano S, Toh-e A, Kuroiwa T (1995) Isolation, characterization and chromosomal mapping of an actin gene from the primitive red alga *Cyanidioschyzon merolae.* Curr Genet **28:** 484–490

Terui S, Suzuki K, Takahiashi H, Itoh R, Kuroiwa T (1995) High synchronization of plastid division in the ultramicro-alga *Cyanidioschyzon merolae* by treatment with both light and aphidicolin. J Phycol **31:** 958–961

Urao T, Yamaguchi-Shinozaki K, Shinozaki K (2000) Two-component systems in plant signal transduction. Trends Plant Sci **5:** 67–74

Vahrenholz C, Riemen G, Pratje E, Dujon B, Michaelis G (1993) Mitochondrial DNA of *Chlamydomonas reinhardtii*: the structure of the ends of the linear 15.8-kb genome suggests mechanisms for DNA replication. Curr Genet **24:** 241–247

Yagisawa F, Nishida K, Okano Y, Minoda A, Tanaka K, Kuroiwa T (2004) Isolation of cycloheximide-resistant mutants of *Cyanidioschyzon merolae.* Cytologia (Tokyo) **69:** 97–100

Yoon HS, Hackett JD, Pinto G, Bhattacharya D (2002) The single, ancient origin of chromist plastids. Proc Natl Acad Sci USA **99:** 15507–15512